Technical Note
Vadose Zone Journal

The Influence of Biofilm Spatial Distribution Scenarios on Hydraulic Conductivity of Unsaturated Soils

Ravid Rosenzweig, Uri Shavit, and Alex Furman*

The development of biofilms in unsaturated soils is likely to influence the hydraulic conductivity function. Despite its importance, this effect has received little attention. Mostafa and Van Geel (2007, *Vadose Zone Journal*, 6:175–185) proposed several hydraulic conductivity models that acount for the effect of bacteria in unsaturated soils. We have expanded these models by considering the change in biofilm pore-size distribution and its effect on the entire hydraulic conductivity function. Three scenarios were considered: (i) the biofilm fills the smallest pores first; (ii) a biofilm of uniform thickness coats all pore walls; and (iii) the biofilm coats the soil with a constant volume fraction of each pore. The results show that the pore-scale distribution of the biofilm has a significant effect on the hydraulic properties of the soil and therefore has to be accounted for when modeling flow and transport in biofilm-affected soils.

Abbreviations: MVG, Mostafa and Van Geel (2007).

Conductivity reduction in soils and aquifers due to bacterial activity has been a subject of growing interest. Numerous works have studied hydraulic conductivity reduction under saturated conditions, also known as *bioclogging*. These works include experimental studies (Okubo and Matsumoto, 1979; Taylor and Jaffe, 1990; Cunningham et al., 1991; Vandevivere and Baveye, 1992) as well as some theoretical studies that proposed conceptual models for the saturated hydraulic conductivity of bacteria-affected soils (Taylor et al., 1990; Vandevivere et al., 1995). These models can be roughly divided into three categories: biofilm models (Taylor et al., 1990), in which the biofilm is modeled as a continuous layer covering the pore walls; microcolony models (Thullner et al., 2002), in which the biofilm is modeled as patches attached to the solid phase; and macroscopic models (Clement et al., 1996), in which no assumptions are made regarding the biofilm distribution within the pores. To date there has been very limited research regarding the effect of bacteria on the soil hydraulic conductivity under unsaturated conditions (Rockhold et al., 2002, 2005; Yarwood et al., 2006).

Recently, Mostafa and Van Geel (2007) (referred to here as MVG) proposed three conceptual models for the description of the effect of bacteria on the unsaturated hydraulic conductivity. The models are based on the formulations of Mualem (1976) and van Genuchten (1980) for the unsaturated hydraulic conductivity and water retention curve, respectively. The first MVG model assumes that biofilms clog the small pores. By using the Mualem (1976) model and integrating the retention function across a truncated pore space, MVG obtained a new expression for the modified hydraulic conductivity function. The second MVG model scales the relative conductivity according to the bacteria-free fraction. Mostafa and Van Geel (2007) pointed out that their second model is a simple scaling relationship that is not based on physical reasoning or experimental results. The third model assumes that the biofilm coats pore capillaries with a layer of uniform thickness. The model uses the capillary model and calculates the ratio between the saturated conductivity of bacteria-affected soil and bacteria-free soil. This ratio is then used to scale the hydraulic conductivity function of bacteria-free soil.

While computing the hydraulic conductivity, all three MVG models adjust the Mualem–van Genuchten relation for the biofilm-free soil to accommodate the bacteria effect. This is done without changing van Genuchten's empirical parameters. The first MVG model modifies the conductivity by limiting the integration range of the retention curve, whereas the second and third

Civil and Environmental Engineering, Technion, Haifa 32000, Israel. *Corresponding author (afurman@technion.ac.il).

Vadose Zone J. 8:1080–1084
doi:10.2136/vzj2009.0017
Received 26 Feb. 2009.
Published online 28 Oct. 2009.

models use scaling, which leads to a reduction of the hydraulic conductivity function without changing in its shape.

In the current work, we followed MVG's third model concept and studied three scenarios in which the biofilm was distributed differently across the pore space. As opposed to MVG, who used the capillary model to calculate the saturated hydraulic conductivities of the bacteria-affected and bacteria-free soils in determining their flow reduction factor, we used the capillary model to modify the pore-size distribution and then calculated the entire hydraulic conductivity function through the capillary flow model. Although MVG considered two biofilm distributions (namely, the biofilm fills the small pores or uniformly coats the pore inner walls), they calculated the conductivity for each scenario differently. We consistently used the same procedure for all the scenarios. We thus could better examine the effect of the biofilm's distribution on the resulting conductivities and estimate its significance in controlling the hydraulic properties of biofilm-affected soils.

Theory

We followed MVG by considering a soil with a volume fraction θ_m [-] ($\theta_m = V_m/V_{total}$, where V_m is the volume occupied by the biofilm and V_{total} is the total volume of soil) occupied by biofilm, as illustrated in Fig. 1. The biofilm contains solids as well as large amounts of water, which can be found both in the cells and in the surrounding polymeric matrix. We define a microbial effective saturation Se_m [-] as

$$Se_m = \frac{Sa_m}{1-S_{wr}} = \frac{\theta_m}{\theta_s - \theta_r} \quad [1]$$

where $Sa_m = \theta_m/\theta_s$ [-] is the actual microbial saturation, $S_{wr} = \theta_r/\theta_s$ [-] is irreducible water saturation, and θ_s [-] and θ_r [-] are the saturated and irreducible water contents, respectively. The saturated water content is defined by the volume ratio, $\theta_s = (V_{air} + V_w + V_m)/V_{total}$ (Fig. 1), and the effective water saturation Se_w [-] is

$$Se_w = \frac{Sa_w - S_{wr}}{1-S_{wr}} = \frac{\theta_w - \theta_r}{\theta_s - \theta_r} \quad [2]$$

where θ_w [-] is the (mobile) water content and $Sa_w = \theta_w/\theta_s$ [-] is the actual water saturation. Note that in the presence of bacteria, water saturation is always <1.

The capillary model is a simplistic conceptual representation of the soil behavior in terms of water flow and retention. Above all, it provides a simple physical tool to demonstrate the relations between the pore-size distribution and hydraulic properties, and thus it is especially useful in comparative studies.

For clarity, we begin with a short description of the capillary model. The model assumes that the soil pores are represented by bundles of capillary tubes of various diameters. The pores can be either empty or filled with water depending on the capillary head (i.e., matric potential head), such that the effective radius of the largest water-filled capillary is

$$r = -\frac{2\sigma\cos\beta}{\gamma h} \quad [3]$$

where h is the (negative) capillary head [L], σ [M T^{-2}] is the surface tension (0.072 N m^{-1} for distilled water at 20°C), γ [M L^{-2} T^{-2}] is the specific weight, and β [-] is the water contact angle with the tube walls, commonly assumed to be zero. Given a known soil-water retention curve, the pore-size distribution can be found by dividing the interval between θ_r and θ_s into M segments of $\Delta\theta$ each, with each segment representing a group i of capillaries with an effective radius of r_i and a density number $N_i = \Delta\theta/\pi r_i^2$ [L^{-2}].

The hydraulic conductivity can then be computed by using the Hagen–Poiseuille equation for laminar flow in a tube:

$$K\left[\theta = \theta_s - (M-j)\Delta\theta\right] = \frac{\tau\gamma\pi}{8\mu}\sum_{i=1}^{j} N_i r_i^4 = \frac{\tau\Delta\theta\sigma^2}{2\gamma\mu}\sum_{i=1}^{j}\frac{1}{h_i^2} \quad [4]$$

where μ [M L^{-1} T^{-1}] is the water dynamic viscosity, τ [-] is the tortuosity, and $j = 1{:}M$ is the index of the capillary groups, where $j = 1$ indicates the smallest pore bundle.

We modified the models of MVG by calculating the pore distribution of the biofilm-affected soil according to the capillary model. While MVG used the capillary model to find the ratio between the biofilm-affected and biofilm-free saturated conductivities, we used the capillary model to modify the unsaturated conductivity across the entire saturation range. In the following, we define a relative biofilm-affected unsaturated conductivity as the ratio between the unsaturated conductivity of the biofilm-affected soil and the saturated conductivity of the biofilm-free soil:

$$K_b\left(\theta_{w,j}\right) = \frac{\sum_{i=1}^{j} N_{b,i} r_{b,i}^4}{\sum_{i=1}^{M} N_{f,i} r_{f,i}^4} \quad [5]$$

where **r** [L] and **N** [L^{-2}] are the pore radius and the density number vectors, with the subscripts f and b representing properties of the biofilm-free and biofilm-affected soils, respectively (there are cases where $N_{b,i}$ and $N_{f,i}$ are not identical); $\theta_{w,j} = \theta_r + \pi\sum_{i=1}^{j} N_{b,i} r_{b,i}^2$ is

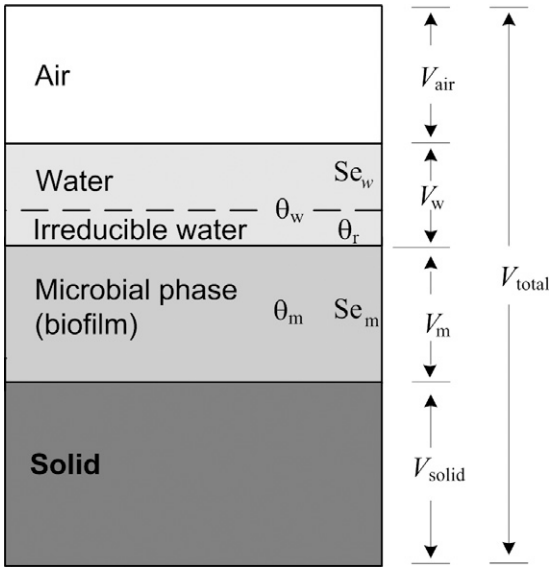

FIG. 1. The different phases of a bacteria-amended soil (V is volume with subscripts for air, water (w), microbial film (m), solid, and total; θ is volume fraction with subscripts for mobile water (w), residual water (r), and the microbial film (m); and Se is effective saturation.

the water content vector ranging from θ_r to $\theta_s - \theta_m$. Note that when $j = M_b$ (where M_b is the number of flow-effective pore groups in the biofilm-affected soil, $M_b \leq M$), the scaling ratio used by the third MVG model is obtained.

Data regarding bacteria distribution within soil pore space are limited because combined soil microstructure and biomass measurements are difficult to obtain. A few studies have attempted to conduct such measurements, leading to contrasting results. For example, Bundt et al. (2001) and Nunan et al. (2003) found high bacterial densities in preferential flow paths. These flow paths usually consist of macropores rather than small pores. On the other hand, Ranjard and Richaume (2001) reported high bacterial densities in microaggregates.

The third MVG model examines a biofilm of a uniform thickness. We expanded this model by examining three cases as described in Fig. 2. In the first (R1), the bacteria fills the smallest pores (as in the first model of MVG). The second (R2) implements the concept of the MVG third model and considers a uniform biofilm thickness in all pores. In our third model (R3), the biofilm coats the pore walls to fill a constant fraction of the pore volume regardless of its diameter. While in the first two models the smallest pores will be clogged first and the larger pores would not be affected (or would be slightly affected), in the third model the cross-section of all pores will be reduced by the same percentage, regardless of their size.

Thus the pore radii and the density numbers for the R1, R2, and R3 models are

$$r_{b,i} = \begin{cases} r_{f,i} & \frac{\theta_m}{\Delta\theta} < i < M \\ 0 & \text{else} \end{cases} \quad \text{for R1} \qquad [6a]$$

$$r_{b,i} = \begin{cases} r_{f,i} - d & r_{f,i} > d \\ 0 & \text{else} \end{cases} \quad \text{for R2} \qquad [6b]$$

$$r_{b,i} = r_{f,i}\sqrt{1 - Se_m} \quad \text{for R3} \qquad [6c]$$

$$N_{b,i} = \begin{cases} \dfrac{i\Delta\theta - \theta_m}{\pi r_{f,i}^2} & \dfrac{\theta_m}{\Delta\theta} < i < \dfrac{\theta_m}{\Delta\theta} + 1 \\ N_{f,i} & \dfrac{\theta_m}{\Delta\theta} + 1 < i < M \\ 0 & \text{else} \end{cases} \quad \text{for R1} \qquad [7a]$$

$$N_{b,i} = \begin{cases} N_{f,i} & r_{f,i} > d \\ 0 & \text{else} \end{cases} \quad \text{for R2} \qquad [7b]$$

$$N_{b,i} = N_{f,i} \quad \text{for R3} \qquad [7c]$$

where d [L] is the uniform biofilm thickness (in R2), which is iteratively calculated using

$$\theta_m - \sum_{i=1}^{j-1} N_{f,i}\pi r_{f,i}^2 = \sum_{i=j}^{M}\left[N_{f,i}\pi r_{f,i}^2 - N_{f,i}\pi\left(r_{f,i} - d\right)^2\right] \qquad [8]$$

The second term on the left-hand side of Eq. [8] sums those capillaries with a radius smaller than d, which are completely biofilm filled. The value of d is calculated by an iterative search for a value of j such that the rest of the biofilm is distributed in the larger capillaries to reach the value of θ_m.

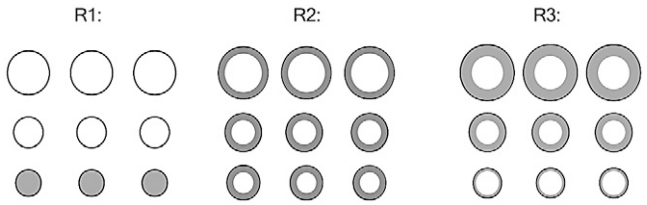

FIG. 2. The three scenarios of the tested biofilm spatial distributions: R1, the biofilm fills the small pores first; R2, the biofilm coats all pores with a layer of uniform thickness; R3, the biofilm covers a constant fraction of each pore cross-section.

For each of the three cases, the relative unsaturated conductivity is calculated separately using Eq. [5]. The results of our three models along with the results of MVG are reported in the following.

Results and Discussion

The performance of the different models was examined by considering two representative soils: a sand and a loam (Carsel and Parrish, 1988). The soil hydraulic properties including the saturated conductivity, K_s [L T^{-1}], the water contents θ_s and θ_r, and the van Genuchten constants α and n are listed in Table 1. The two soils have different pore-size distributions. While the pore-size distribution within the sand is relatively uniform, the loam exhibits a more graded pore structure. For each soil, the unsaturated hydraulic conductivity profiles were calculated using Eq. [5–7] for two microbial saturations (Se_m): 0.2 and 0.6. Pore-size distributions of the biofilm-free soils were obtained from the retention curves generated by the van Genuchten formulation (van Genuchten, 1980) using the empirical parameters given in Table 1.

Table 2 describes the statistical properties of the modified pore-size distributions that were obtained by our three models (Eq. [6] and [7]). These distributions are described in terms of the dimensionless flow-weighted mean radius, $\overline{r}_w^*$, and the dimensionless standard deviation, σ_w^*:

$$\overline{r}_{w,k}^* = \frac{\overline{r}_{w,k}}{\overline{r}_{w,f}} \qquad [9]$$

where $\overline{r}_{w,k}$ [L] and $\overline{r}_{w,f}$ [L] are the weighted mean radii of the biofilm-affected soil obtained by the Rk model (where k = 1, 2, or 3) and the biofilm-free soil, respectively; $\overline{r}_w$ is defined as

$$\overline{r}_w = \left(\frac{\sum_{i=1}^{M} N_i r_i^4}{\sum_{i=1}^{M} N_i}\right)^{0.25} \qquad [10]$$

TABLE 1. Properties of the van Genuchten relation for the tested soils (Carsel and Parrish, 1988). Values of saturated hydraulic conductivity (K_s) are presented for completeness.

Parameter†	Sand	Loam
n	2.68	1.56
α, m^{-1}	14.5	3.6
θ_s	0.43	0.43
θ_r	0.045	0.078
K_s, m d^{-1}	7.128	0.249

† θ_s, saturated volumetric water content; θ_r, residual volumetric water content; α and n, constants.

TABLE 2. Statistical properties of the modified pore-size distributions for microbial effective saturations (Se_m) of 0.2 and 0.6.

Model	Parameter†	Sand		Loam	
		Se_m = 0.2	Se_m = 0.6	Se_m = 0.2	Se_m = 0.6
R1	$\overline{r}_w^*$	1.90	2.90	37.48	96.19
	σ_w^*	0.55	0.40	0.85	0.64
R2	$\overline{r}_w^*$	1.20	1.47	19.24	49.00
	σ_w^*	0.94	0.89	0.96	0.90
R3	$\overline{r}_w^*$	0.89	0.63	0.89	0.63
	σ_w^*	1	1	1	1

† $\overline{r}_w^*$, dimensionless flow-weighted mean radius; σ_w^*, dimensionless standard deviation.

The flow-weighted mean radius reflects the contribution of the different pore radii to the conductivity (see Eq. [4]), and thus gives small pores a lower weight in calculating $\overline{r}_w$ with respect to larger pores. The corresponding dimensionless standard deviation, σ_w^*, is expressed as

$$\sigma_{w,k}^* = \frac{\sigma_{w,k}/\overline{r}_{w,k}}{\sigma_{w,f}/\overline{r}_{w,f}} \quad [11]$$

where $\sigma_{w,k}$ [L] and $\sigma_{w,f}$ [L] are the standard deviations (with respect to r_w) of the biofilm-affected soil obtained by the R*k* model and the biofilm-free soil, respectively.

The effect of the different models on the pore-size distribution is shown in Table 2. The influence of the clogged pore space results in $\overline{r}_{w,1}^* > \overline{r}_{w,2}^* > \overline{r}_{w,3}^*$, which is a direct result of the truncated pore space in R1 and R2. As demonstrated in Fig. 2, the small pores are excluded by R1. In R2, the pores' diameter is reduced and as a result the pores whose diameters are smaller than *d* are also excluded. Note that in R3 the dimensionless flow-weighted mean radius is $\overline{r}_{w,3}^* = \sqrt{1-Se_m}$ (Eq. [6c]), and as a result the mean radius is smaller than in the original biofilm-free case. The degree of pore space truncation affects also the standard deviation. The R1 model, which results in the biggest truncation of small capillaries, yields the smallest $\sigma_{w,k}^*$ values. Since small capillaries in R2 are not necessarily eliminated but their diameter is reduced, the $\sigma_{w,k}^*$ values are higher. The dimensionless standard deviation in R3 equals one because all the pores are scaled in the same way. Table 2 also demonstrates the different results obtained for the two soils. Since sand has a relatively uniform pore-size distribution and loam is more graded, the effect of the R1 and R2 models on the loam is more pronounced.

The modified pore-size distributions enable calculating the new water retention curves of the biofilm-affected soils. As these curves are not an intermediate step in the process of calculating the hydraulic conductivity, however, they are not shown here.

Figure 3 presents the conductivity of the biofilm-free soil (computed by Eq. [4]) and the conductivities obtained by our three models (R1–R3) as a function of θ_w. Since MVG did not provide such plots for their models, we include the conductivity function of their first model. We chose not to present the results of the second and third MVG models since they scale the conductivity of the biofilm-free soil by a factor smaller than one, and thus are expected to yield similar profiles to those of the biofilm-free soil but with lower values.

Somewhat counterintuitively, the conductivity obtained for all models (for a given water content) was consistently higher than the conductivity of the biofilm-free soil. We note that, unlike in the saturated case, where water fills the entire pore space and the biofilm-affected conductivity has to be smaller than the biofilm-free conductivity, in the unsaturated case the situation is different. As the biofilm fills some of the pore volume, it primarily influences the small pores. Thus, the free water is reallocated into larger pores, which results in a higher hydraulic conductivity. Because the larger pores govern the flow, the amount of water diverted into these pores will control the change in hydraulic conductivity due to biofilm growth. It can be seen that the R1 model, which assumes that the biofilm occupies the smallest pores and therefore causes the largest shift of water to larger pores, results in the highest conductivity. Next is the R2 model, which assumes that the biofilm coats the pore walls with a uniform biofilm layer and therefore also influences mostly the smallest pores, but to a lesser extent than the R1 model. The

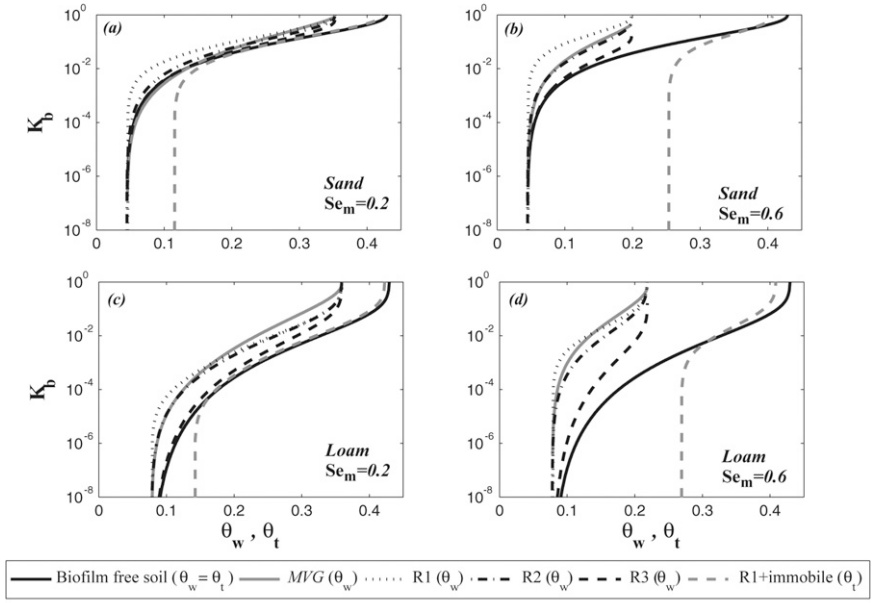

FIG. 3. Relative hydraulic conductivity functions obtained by the R1, R2, and R3 models, by the first model of Mostafa and Van Geel (2007) (MVG), and by introducing an immobile water phase to R1 (R1 + immobile). The results are also compared with the hydraulic conductivity function of the biofilm-free soil. Four cases were tested: (a) sand, microbial effective saturation (Se_m) = 0.2; (b) sand, Se_m = 0.6; (c) loam, Se_m = 0.2; (d) loam, Se_m = 0.6. While the conductivity profiles in the R1 to R3 and MVG models are presented as a function of the mobile water content (θ_w), the conductivity of the R1 + immobile model is plotted as a function of the total water content, θ_t. Note that in the biofilm-free profile, $\theta_w = \theta_t$.

conductivity function generated by the third model, R3, yields smaller values in comparison to both R1 and R2 and is the closest to the conductivity profile computed for the biofilm-free soil. This stems from the uniform biofilm distribution across the pore space (i.e., a constant fraction of each pore is filled with biofilm), which leads to a smaller shift of water toward larger pores. The conductivity profiles that result from the first MVG model lie within the range of the R1 and R2 models. This is expected because the first MVG model and our R1 model are based on the same concept (preferential clogging of the smallest pores).

The difference in the effect of the various models on the two soils is clearly seen. Whereas the effect of the models on the sand is relatively mild, it is more pronounced in the loam. This is due to the more significant modification in the pore-size distribution of the loam than the sand, as was explained above.

Up to this point, we have focused on the mobile water phase while ignoring the bound water within the biofilm. It is well known that a biofilm is a well hydrated environment that can absorb a large amount of water (Roberson and Firestone, 1992). The water fraction within the biofilm is often considered as an immobile water phase (Or et al., 2007). Thus, the total water content, θ_t, at a specific hydraulic conductivity includes the biofilm immobile water:

$$\theta_t = \theta_{im} + \theta_w \quad [12]$$

Accounting for the biofilm immobile water is important because laboratory methods for measuring the water content, such as the gravimetric method and presumably time domain reflectometry, measure the total water content. On the other hand, only the mobile water contributes to flow. We chose to include the immobile water phase by conservatively assuming that 90% of the biofilm volume is occupied by water ($\theta_{im} = 0.9\theta_m$). Figure 3 shows an additional curve that represents a combination of this immobile water concept and the R1 model (R1 + immobile). Note that while in the R1 to R3 and MVG models the conductivity is presented as a function of θ_w, the R1 + immobile profile is a function of θ_t, given by Eq. [12]. Since in the biofilm-free soil the microbial phase is absent, $\theta_w = \theta_t$. When the biofilm immobile water is included, the conductivity profiles of the biofilm-affected soils and the profiles of the biofilm-free soils are similar for high water content. For lower water content, θ_t approaches $\theta_{im} + \theta_r$ and a deviation from the profile of the biofilm-free soil is observed. Although the total water content in this region is still high, the water is bound and cannot contribute to the hydraulic conductivity. In fact, our results for this region are in agreement with flow measurements in biofilm-amended sand columns obtained recently by Rol (2007). It was found that as the unsaturated hydraulic conductivity was reduced, the total water content was moderately increased.

In the current work, we expanded the work of Mostafa and Van Geel (2007) by examining the effect of biofilm distribution within the pore space and testing synthetic models of biofilm-affected soils to obtain their unsaturated hydraulic conductivity functions. The results show that the spatial distribution of the biofilm has a significant effect on the hydraulic properties of the soil. We therefore concluded that the pore-scale phenomenon needs further research to provide evidence of the biofilm distributions, which will lead to a better choice of models for the hydraulic properties of biofilm-affected soils.

Acknowledgments

We would like to acknowledge the Star–Gilbert Memorial Fund for their generous financial support.

References

Bundt, M., F. Widmer, M. Pesaro, J. Zeyer, and P. Blaser. 2001. Preferential flow paths: Biological 'hot spots' in soils. Soil Biol. Biochem. 33:729–738.

Carsel, R.F., and R.S. Parrish. 1988. Developing joint probability distributions of soil water retention characteristics. Water Resour. Res. 24:755–769.

Clement, T.P., B.S. Hooker, and R.S. Skeen. 1996. Macroscopic models for predicting changes in saturated porous media properties caused by microbial growth. Ground Water 34:934–942.

Cunningham, A.B., W.G. Characklis, F. Abedeen, and D. Crawford. 1991. Influence of biofilm accumulation on porous media hydrodynamics. Environ. Sci. Technol. 25:1305–1311.

Mostafa, M., and P.J. Van Geel. 2007. Conceptual models and simulations for biological clogging in unsaturated soils. Vadose Zone J. 6:175–185.

Mualem, Y. 1976. New model for predicting hydraulic conductivity of unsaturated porous media. Water Resour. Res. 12:513–522.

Nunan, N., K.J. Wu, I.M. Young, J.W. Crawford, and K. Ritz. 2003. Spatial distribution of bacterial communities and their relationships with the microarchitecture of soil. FEMS Microbiol. Ecol. 44:203–215.

Okubo, T., and J. Matsumoto. 1979. Effect of infiltration rate on biological clogging and water quality changes during artificial recharge. Water Resour. Res. 15:1536–1542.

Or, D., S. Phutane, and A. Dechesne. 2007. Extracellular polymeric substances affecting pore-scale hydrologic conditions for bacterial activity in unsaturated soils. Vadose Zone J. 6:298–305.

Ranjard, L., and A.S. Richaume. 2001. Quantitative and qualitative microscale distribution of bacteria in soil. Res. Microbiol. 152:707–716.

Roberson, E.B., and M.K. Firestone. 1992. Relationship between desiccation and exopolysaccharide production in a soil *Pseudomonas* sp. Appl. Environ. Microbiol. 58:1284–1291.

Rockhold, M.L., R.R. Yarwood, M.R. Niemet, P.J. Bottomley, and J.S. Selker. 2002. Considerations for modeling bacterial-induced changes in hydraulic properties of variably saturated porous media. Adv. Water Resour. 25:477–495.

Rockhold, M.L., R.R. Yarwood, M.R. Niemet, P.J. Bottomley, and J.S. Selker. 2005. Experimental observations and numerical modeling of coupled microbial and transport processes in variably saturated sand. Vadose Zone J. 4:407–417.

Rol, J. 2007. Biofilm formation in unsaturated soil. Hebrew Univ., Rehovot, Israel.

Taylor, S.W., and P.R. Jaffe. 1990. Biofilm growth and the related changes in the physical properties of a porous medium: 1. Experimental investigation. Water Resour. Res. 26:2153–2159.

Taylor, S.W., P.C.D. Milly, and P.R. Jaffe. 1990. Biofilm growth and the related changes in the physical properties of a porous medium: 2. Permeability. Water Resour. Res. 26:2161–2169.

Thullner, M., L. Mauclaire, M.H. Schroth, W. Kinzelbach, and J. Zeyer. 2002. Interaction between water flow and spatial distribution of microbial growth in a two-dimensional flow field in saturated porous media. J. Contam. Hydrol. 58:169–189.

Vandevivere, P., and P. Baveye. 1992. Saturated hydraulic conductivity reduction caused by aerobic bacteria in sand columns. Soil Sci. Soc. Am. J. 56:1–13.

Vandevivere, P., P. Baveye, D.S. Delozada, and P. Deleo. 1995. Microbial clogging of saturated soils and aquifer materials: Evaluation of mathematical models. Water Resour. Res. 31:2173–2180.

van Genuchten, M.Th. 1980. A closed-form equation for predicting the hydraulic conductivity of unsaturated soils. Soil Sci. Soc. Am. J. 44:892–898.

Yarwood, R.R., M.L. Rockhold, M.R. Niemet, J.S. Selker, and P.J. Bottomley. 2006. Impact of microbial growth on water flow and solute transport in unsaturated porous media. Water Resour. Res. 42:W10405, doi:10.1029/2005WR004550.